PTENP1: A Pivotal Pseudogene in Glioblastomas

Sammy Mustafa

ABSTRACT

Glioblastoma multiforme (GBM) is the most prevalent and malignant brain tumor in the adult population. Aberrant activation of the PI3K/Akt pathway results in the proliferation of GBMs. The phosphatase and tensin homolog (PTEN) protein functions as a tumor suppressor by attenuating Akt activation. However, most GBMs demonstrate PTEN mutations and deletions. This may be due to the high expression of microRNA-26a (miR-26a) in GBMs. miR-26a binds to the 3'-UTR of PTEN and subsequently represses PTEN. To combat miRNA repression, pseudogenes like PTENP1 are studied. While mutations prevent PTENP1 from producing functional proteins, PTENP1 remains highly homologous to its parent gene, PTEN. This allows PTENP1 to have a role in gene regulation by competitively binding to the miRNAs of its target gene, like miR-26a. Since PTENP1 is highly homologous to PTEN, upregulating PTENP1 may serve as a potential chemotherapy for GBMs. After PTENP1 was upregulated in the GBM cell line T98G, decreased PTEN and miR-26a levels decreased and proliferation was inhibited ($p<0.001$). Interestingly, Akt levels increased ($p<0.05$) and subsequent ELISAs suggested dual inhibition and activation of the PI3K/Akt pathway. PTENP1 overexpression demonstrated enhanced sensitivity to TMZ treatment ($p<0.001$). Moreover, cell cycle arrest was induced in G0/G1 and autophagy increased ($p<0.001$). Also, the potential of angiogenesis significantly reduced and migration was subsequently inhibited. Taken together, the findings suggest PTENP1 overexpression as a novel modulator of the malignancy of GBMs.

INTRODUCTION

Gliomas are the most prevalent malignant brain tumor in the adult population, encompassing 81% of all malignant brain tumors. Moreover, glioblastoma multiforme (GBM) is the most common and aggressive variant of gliomas with an average survival time of 1.5 years (Li et al., 2015). Although advancements have been made in the treatment of GBMs, this tumor remains one of the deadliest and treatment-resistant tumors of any cancer. Hence, the development of more effective therapies requires a deeper understanding of the cellular and molecular pathways which prevail in GBMs.

The etiology of GBMs is often traced back to the PI3K/Akt pathway. In fact, the PI3K/Akt is over-activated in around 90% of all GBMs (Langhans et al., 2017). More specifically, the activation of Akt promotes GBM survival, proliferation, migration, and angiogenesis (Wang et al. 2019). In response, the phosphatase and tensin homolog (PTEN) protein functions as a tumor suppressor by attenuating Akt activation. Thus, the role of PTEN in GBM is crucial in the context of the PI3K/Akt pathway and preventing gliomagenesis.

However, 75% of gliomas have reported PTEN mutations or deletions (De Luca et al., 2012). GBM research suggests this may be due to microRNAs (miRNAs), small endogenous RNAs that bind to the 3′-UTR of mRNAs to repress translation (Ruegger & Großhans, 2012). Interestingly, it has been reported that miR-26a is overexpressed in high-grade gliomas and directly targets PTEN (Huse et al., 2009). This means that miR-26a silences PTEN translationally and subsequently activates the PI3K/Akt pathway, promoting GBM progression (Figure 1). Moreover, miR-26a induces the resistance to the first line treatment for GBMs: temozolomide (TMZ) (Get et al., 2018). With this in mind, miR-26a can be considered an oncomiR in gliomas.

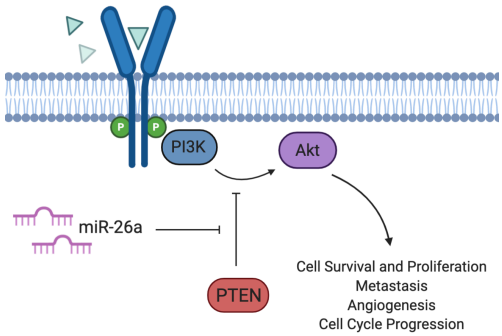

Figure 1: Basic overview of the PI3K/Akt pathway and miR-26a in GBMs. PI3K/Akt pathway activation causes gliomagenesis. PTEN inhibits phosphorylation, inhibiting Akt activation. miR-26a directly targets PTEN. Figure created by author.

More recent research finds constitutive genes that can function to target miRNAs: pseudogenes. Pseudogenes are genes that lack the ability to produce functional proteins due to coding-sequence deficiencies like frameshifts and premature stop codons. While pseudogenes were previously viewed as nonfunctional “junk” cluttering the human genome, pseudogenes have recently been recognized for their essential roles in gene regulation. This may be due to the high resemblance pseudogenes have with their parent genes. Of note, PTENP1 is regarded as the pseudogene of the PTEN gene. It has been reported that the PTENP1 3’-UTR is 95% homologous to that of PTEN (Poliseno et al., 2010). This indicates the miR-26a binding sites on the 3’-UTR of PTEN are homologous to the 3’-UTR of PTENP1. This suggests that miR-26a can competitively bind to both PTEN and PTENP1 (Figure 2). The high homology between the

3'UTR in PTEN and PTENP1 suggests PTENP1 may act as a "decoy" for miR-26a binding, liberating PTEN from miR-26a repression and enabling PTEN to carry out its function as a tumor suppressor.

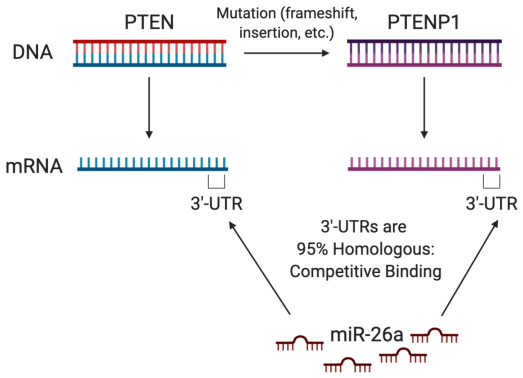

Figure 2: Basic overview of the PTEN pseudogene. PTENP1 evolved from PTEN due to coding-sequence deficiencies. The 3'UTR of PTENP1 is highly homologous to that of PTEN, allowing miR-26a to competitively bind to both. Figure created by author.

Because of the complex interactions between the PTEN, PTENP1, miR-26a, and the PI3K/Akt pathway, little improvement has been made toward the development of treatments for these high-grade brain tumors. In the research reported here, the upregulation of PTENP1 was utilized to determine the underpinnings of the interactions of these molecules in GBMs. It was hypothesized that PTENP1 overexpression ($PTENP1^{+}$) would result in an increase in PTEN gene expression, inhibiting the PI3K/Akt signaling pathway and leading to GBM cell death. An understanding of the signal transduction pathways involved with increased expression of PTENP1 could potentially indicate a novel approach for targeting GBMs.

MATERIALS AND METHODS

Cell culture and reagents

The human glioblastoma multiforme cell line T98G (ATCC, Manassas, VA) was cultured in Dulbecco's Modified Eagle Medium (Invitrogen, Grand Island, NY), supplemented with 10% FBS and 1% penicillin-streptomycin (Invitrogen). Cells were incubated at 37°C and 5% CO_2. When confluent, the cells were trypsinized using 0.05% trypsin-EDTA (Invitrogen).

Stable Transfection with PTENP1 plasmid

Cells were transfected with PTENP1 plasmid (Origene, Rockville, MD) for $PTENP1^{+}$ cells and an empty vector for control cells, according to the Origene protocol for DNA plasmid transfection.

qRT-PCR

RNA was isolated and purified from the Control and $PTENP1^{+}$ cells using the RNeasy Plus Mini Kit (Qiagen, Germantown, MD). The Power SYBR® Green RNA-to-CT™ 1-Step Kit (Thermo Fisher Scientific, Waltham, MA) was utilized to measure PTENP1 and PTEN mRNA levels. The qSTAR miRNA qPCR Detection System (OriGene, Rockville, MD) was used to measure miR-26a levels. Data was analyzed using the ΔΔCq method, to determine the fold increase/decrease of PTENP1, PTEN, and miR-26a expression in the $PTENP1^{+}$ cells.

Preparation of Lysates

Control and PTENP1^{+} cells were trypsinized and centrifuged (7min at 1200rpm). The cell pellets were resuspended in 2mL PBS (Invitrogen) and centrifuged (7min at 1200rpm). Cells were resuspended in 1X lysis buffer #9803 (Cell Signaling Technology, Danvers, MA) supplemented with protease cocktail inhibitor #P8340 (Sigma, St. Louis, MO) at 1x10^{6} cells per 1mL solution. Samples were placed on ice for 10min and then centrifuged (13,000rpm for 15min at 4°C). Lysates were collected and stored at -80°C.

Indirect ELISA

100µL lysate samples in a 96-well ELISA plate were incubated overnight at 4°C. The plate was emptied. 300µL 1X BSA Diluent/Blocking Solution (KPL, Gaithersburg, MD) was used to block wells. A rabbit anti-human primary antibody (1:300) against IL-6 (ab6672, Abcam, Cambridge, MA), pFAK (ab38458, Abcam), pAkt (ab66138, Abcam), pp53 (ab38497, Abcam), pCREB (orb14956, Biorbyt, San Francisco, California), GSKβ phosphorylated at Y216 (ab85305, Abcam), pβ-catenin (ab53050, Abcam), c-Myc (ab39688, Abcam), or LC3 (ab58610, Abcam) was added to wells (1h at RT). After a wash with 1X wash solution (KPL), a horseradish peroxidase labeled goat anti-rabbit IgG antibody (KPL) (1:300) was added to wells (1h at RT). After a wash, 100µL TMB substrate solution (KPL) was added to wells. Absorbance at 405nm was measured (BioTek ELx808 microplate reader, Winooski, VT).

Cell Proliferation Assay

100µL of Control and PTENP1^{+} cells were plated in a 96-well plate at 0.1x10^{6} cells/mL. After 24h, cells were treated with TMZ (100-500µM) (TCI America, Portland, OR, USA). Cell proliferation was measured after 72h, using an MTS assay. 15µL Cell Titer® 96 AQueous One Solution Reagent (Promega, Madison, WI) was added to wells. After 1h incubation, absorbance was measured at 490nm.

Cell Cycle Analysis

After 72h TMZ treatment, manufacturer's protocol was followed to analyze cell cycle progression by flow cytometry (ThermoFisher). Briefly, cells were centrifuged into a pellet, washed with cold PBS, and resuspended in cold binding buffer at 1x10^{6} cells/mL. The resuspended solution was then centrifuged and resuspended with cold PBS. After the addition of 100µg/mL propidium iodide, cells were incubated in the dark for 15 min. Fluorescence was analyzed via flow cytometry with the acquisition criteria of 10,000 events per sample (Cell Lab Quanta SC, Beckman Coulter).

Autophagy Detection Assay

The Autophagy/Cytotoxicity Dual Staining Kit (CayMan Chemical, Ann Arbor, MI) was utilized. Briefly, Control and PTENP1^{+} cells were plated at 5x10^{4} cells/well in a 96-well black culture plate. After 24h, the cells were treated TMZ (400µM). After 72h, cells were stained with a solution consisted of Monodansylcadaverine (MDC) and Propidium Iodide Solution (PI) diluted in Assay Buffer. After a wash with Assay Buffer, cells were analyzed and imaged at 100X. Autophagic vacuole staining was measured at 335/512 nm; cell death was measured at 536/617 nm.

Vascular-Endothelial Tube Formation Assay

EA.hy926 vascular-endothelial cells (ATCC) were cultured in Endothelial Basal Medium (Invitrogen). Membrane Extract (BME) (Cultrex, Minneapolis, MN) was thawed in an ice bath and placed at 4°C overnight. Simultaneously, endothelial cells were treated with the secretome of the Control cells or the secretome of the PTENP1^{+} cells. Following 24h thawing, the BME solution was aliquoted into a 96-well plate at 50 µL per well followed by incubation for 60 min. The cells were plated in a 96-well plate atop the gelled BME. After 4h, vascular-endothelial tube formation was visualized and imaged. Total tube length, branching points, loops, and nets were measured from 4 randomly selected images per group using Wimasis Image Analysis.

Transwell Migration Assay

A migration assay was performed using a 8 µm pore Transwell inserts (353182, Falcon, Corning, NY). Briefly, Transwell inserts were coated with 1% rattail collagen (Invitrogen) in 0.02 N acetic acid (Sigma). Cells were plated in serum free media at 0.1x10^6 cells/mL into each insert in a 12-well plate. Cells were allowed to migrate for 24h towards media with serum. Migrated cells were stained with Giemsa and imaged at 1000X using a phase-contrast microscope.

RESULTS AND DISCUSSION

Stable Transfection of Glioma Cells with PTENP1 Plasmid

After a qRT-PCR was performed, the data were interpreted using the ΔΔCq method. PTENP1^{+} cells demonstrated an 82% overexpression efficiency in PTENP1 mRNA levels compared to the Control cells (Table 1). The 1.82-fold increase in PTENP1 expression indicated a successful transfection with the PTENP1 DNA plasmid. Based on this result, a stable transfection of PTENP1^{+} cells were used for subsequent assays and procedures.

Sample	Mean Cq (GAPDH)	Mean Cq (PTENP1)	Mean ΔCq	Mean ΔCq Expression	ΔΔCq Expression	% OE
Control	18.70	22.28	3.58	0.08362	1	
PTENP1	18.28	21.00	2.72	0.1518	1.82	81.50

Table 1: Percent PTENP1 mRNA Level Overexpression. RNA was isolated from Control and PTENP1^{+} cells and subsequently used to synthesize cDNA. A qRT-PCR was performed to measure PTENP1 mRNA levels. The percent overexpression of PTENP1 mRNA was found to be 81.50%.

miR-26a Downregulation Following PTENP1 Overexpression in Glioma Cells

miR-26a levels were measured to display the effects of PTENP1 overexpression on a PTEN-targeting miRNA. It is reported that there is a direct relationship between miR-26a and IL-6 levels in GBMs (Chen et al., 2016); thus, IL-6 serves as a marker for miR-26a expression. PTENP1^{+} cells demonstrated a significant decrease in IL-6 expression (Figure 3). This indicated that miR-26a expression significantly

decreased following PTENP1 overexpression. To validate the observed decrease in miR-26a expression, a qRT-PCR was performed. The data were analyzed using the ΔΔCq method. PTENP1^{+} cells demonstrated a 69% knockdown efficiency in miR-26a levels compared to the Control cells (Table 2). The 3.24-fold decrease in miR-26a expression indicated that PTENP1 is involved in downregulating miR-26a levels in GBMs.

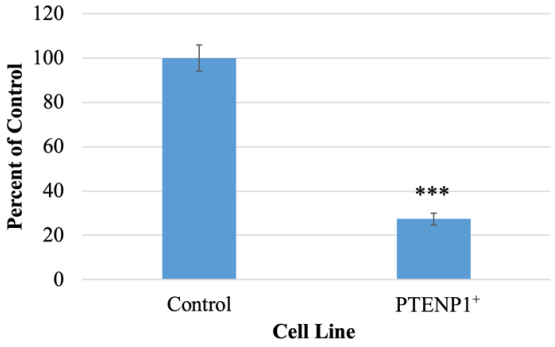

Figure 3: The Effect of PTENP1 Overexpression on IL-6. An indirect ELISA was performed to measure IL-6 in Control and PTENP1^{+} cells. Bars are means +/- STDEV. (n=5). ***=p<0.001.

Sample	Mean Cq (U6)	Mean Cq (miR-26a)	Mean ΔCq	Mean ΔCq Expression	ΔΔCq Expression	% KD
Control	30.37	36.40	6.03	0.01527	1	
PTENP1	27.48	35.21	7.73	0.004710	0.3085	69.15

Table 2: Percent miR-26a Level Knockdown. RNA was isolated from Control and PTENP1^{+} cells and was subsequently used to synthesize cDNA. A qRT-PCR was performed to measure miR-26a levels. The percent knockdown of miR-26a was found to be 69.15%.

PTEN Upregulation Following PTENP1 Overexpression in Glioma Cells

PTEN levels were measured to confirm miR-26a as PTEN-targeting miRNA. After a qRT-PCR was performed, the data were analyzed using the ΔΔCq method. PTENP1^{+} cells demonstrated a 71% overexpression efficiency in PTEN mRNA levels compared to the Control cells (Table 3). The 1.71-fold increase in PTEN expression indicated that PTENP1 is involved in upregulating PTEN levels in glioma cells. This result suggested an upregulation of PTEN following PTENP1 overexpression. Moreover, this result suggested that decreased miR-26a levels correlate with increased PTEN from miRNA-mediated repression.

Sample	Mean Cq (GAPDH)	Mean Cq (PTEN)	Mean ΔCq	Mean ΔCq Expression	ΔΔCq Expression	% OE
Control	18.70	20.64	1.94	0.2606	1	
PTENP1	18.28	19.45	1.17	0.4444	1.71	70.53

Table 3: Percent PTEN mRNA Level Overexpression. RNA was isolated from Control and PTENP1^{+} cells and subsequently used to synthesize cDNA. A qRT-PCR was performed to measure PTEN mRNA levels. The percent overexpression of PTEN was found to be 70.53%.

Aberrant Modulation of the PI3K/Akt Pathway Following PTENP1 Overexpression in Glioma Cells

PTEN is heavily involved in modulating the PI3K/Akt pathway via Akt inhibition (Figure 4). With this in mind, indirect ELISAs were performed to measure PTENP1's effect on various proteins regulating the PI3K/Akt pathway (Figure 5). pFAK levels were not significantly altered in the PTENP1^{+} cells. This may

be due to PTEN modulating the PI3K/Akt pathway downstream of FAK. Interestingly, pAkt levels significantly increased in the PTENP1^{+} cells despite PTEN upregulation ($p<0.05$). Moreover, PTENP1^{+} cells demonstrated a significant decrease in pp53 and pCREB levels ($p<0.05$). While the observed decrease in pp53 levels reinforced the observed upregulation of pAkt, it has been reported that p53 upregulates miR-26a (Lezina et al., 2013). Moreover, the observed decrease in pCREB levels supported the upregulation of PTEN but research has shown CREB knockdown to silence miR-26a (Tan et al., 2012). Continuing on, PTENP1^{+} cells increased the phosphorylation of GSK3β Y216, which is necessary for GSK3β's complete activation (Goc et al., 2014). Interestingly, PTENP1^{+} cells demonstrated a significant increase in β-catenin and c-Myc expression. Collectively, these data suggested that PTENP1 upregulated PTEN independent of antagonizing Akt. However, when considering a pseudogene's multiple transcripts, this may not be the case.

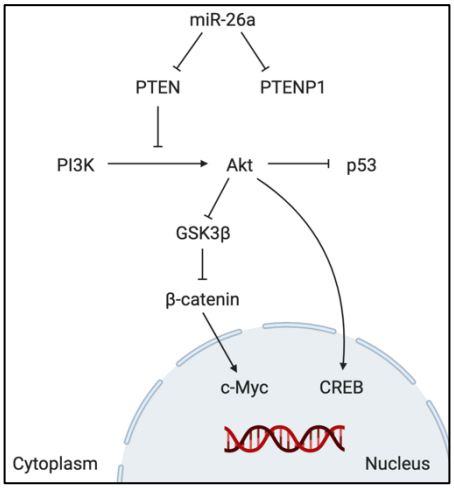

Figure 4: The PI3K/Akt Pathway in Cancer. This diagram illustrates various downstream proteins in the PI3K/Akt signaling pathway in the context of cancer. Figure created by author.

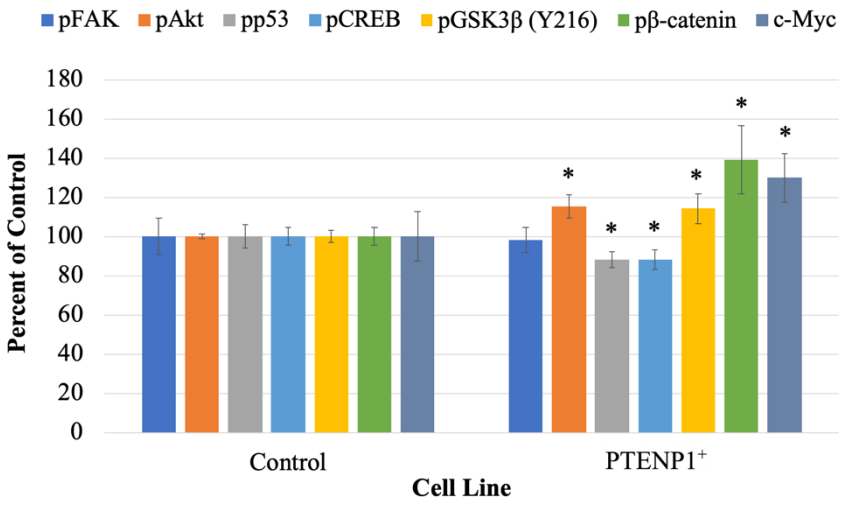

Figure 5: The Effect of PTENP1 Overexpression on the Proteins of the PI3K/Akt Pathway. An indirect ELISA was performed to measure pFAK, pAkt, pp53, pCREB, pGSK3β, pβ-catenin, and c-Myc in Control and PTENP1^{+} cells. Bars are means +/- STDEV. (n=5). *=$p<0.05$.

The Three PTENP1 Transcripts

The existence of multiple PTENP1 transcripts may explain the incongruity between the upregulation of PTEN as well as the increase in pAkt. PTENP1 is transcribed into three transcripts: one sense (S) transcript and two antisense (AS) transcripts (Haddadi et al., 2018). PTENP1(S) acts as a competing endogenous RNA in the cytoplasm, competitively binding to PTEN-targeting miRNAs like miR-26a.

Conversely, PTENP1(AS)α negatively regulates PTEN transcription in the nucleus. However, the PTENP1(AS)β stabilizes the PTENP1(S) transcript through RNA-RNA interactions, strengthening the "miRNA sponge" activity of PTENP1(S) (Figure 6). This suggest that the three PTENP1 transcripts promote pAkt and cytoplasmic PTEN expression. This implies that the PI3K/Akt pathway is both activated and inhibited in different compartments of the cells. Furthermore, observed upregulation and downregulation of certain proteins involved in the PI3K/Akt pathway may be due to the PTENP1 transcripts' cellular location.

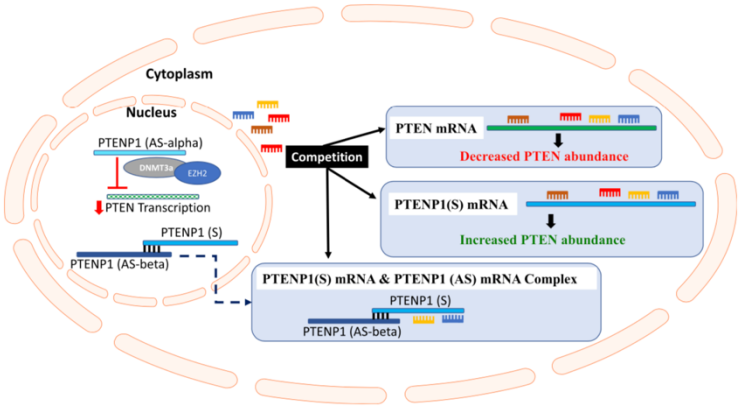

Figure 6: The Three PTENP1 Transcripts (acquired from "PTEN/PTENP1: 'Regulating the regulator of RTK-dependent PI3K/Akt signalling', new targets for cancer therapy", 2018). This diagram displays the location and function of the three PTENP1 transcripts.

The Effect of PTENP1 Overexpression on Cell Viability and Chemosensitivity

While PTENP1 upregulated PTEN tumor-suppressor (Table 3), it allowed for an increase in pAkt involved in tumor proliferation (Figure 5). In addition, the PI3K/Akt pathway has reported roles in TMZ resistance (Li et al., 2017). Thus, cell viability and chemosensitivity were measured (Figure 7). After 72 hours of treatment with various concentrations of TMZ, an MTS assay was performed to assess cell viability and proliferation. Interestingly, the Control cells exhibited a significant decrease in proliferation at 200 µM ($p<0.001$), 400, and 500 µM ($p<0.05$) in spite of expressing MGMT, which confers chemoresistance to TMZ. Also, the Control cells at 100 µM demonstrated no significant change in viability, corroborating the constitutive MGMT-mediated

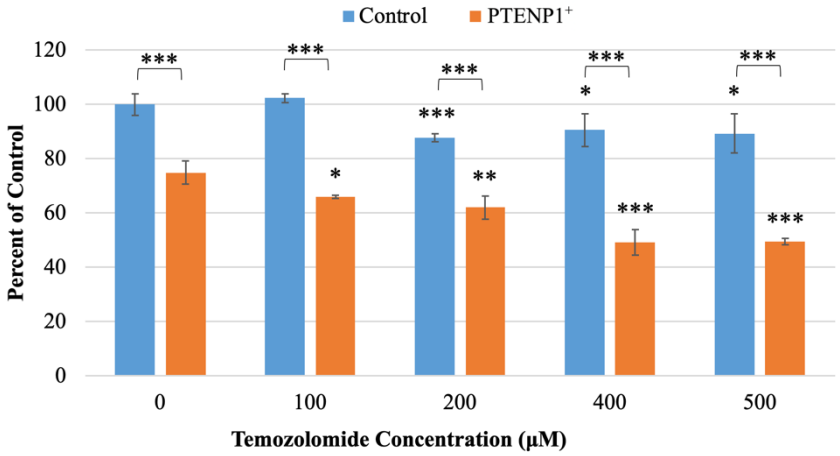

Figure 7: The Effect of PTENP1 Overexpression on Cell Viability and TMZ Sensitivity. Control and PTENP1$^+$ cells were treated with TMZ (100-500 µM). An MTS assay was performed to study the effect of a 72-hour TMZ treatment on cell proliferation and chemosensitivity. Bars are means +/- STDEV. (n=5). *=$p<0.05$, **=$p<0.01$, ***=$p<0.001$.

chemoresistance of the Control cells. Moreover, the cell viability of PTENP1$^+$ cells was consistently lower than that of the Control cells without treatment and at the same TMZ concentration ($p<0.001$). Increasing the TMZ concentration decreased cell viability in PTENP1$^+$ cells in a dose-response fashion, indicating the anti-proliferative potential of TMZ. Taken together, these results suggested reduced cellular proliferation and enhanced chemosensitivity following PTENP1 overexpression in GBMs. Due to 400 µM being the lowest concentration with the greatest significant decrease in cell proliferation in the PTENP1$^+$ cells, 400 µM TMZ was chosen for subsequent assays.

Induced Cell Cycle Arrest Following PTENP1 Overexpression in Glioma Cells

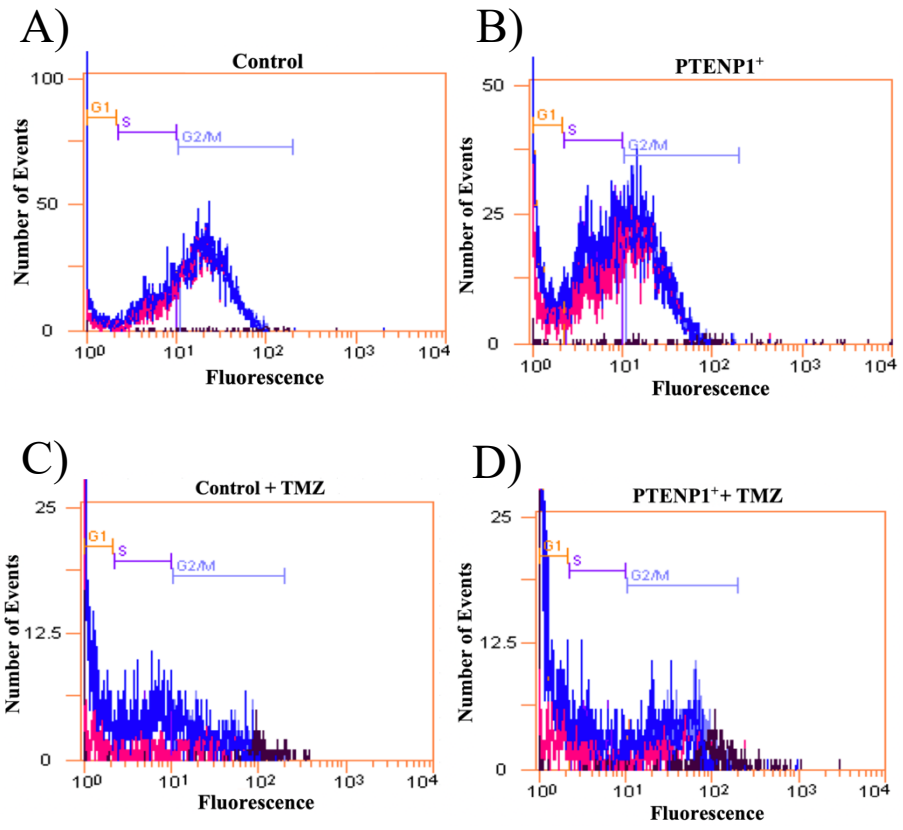

Figure 8: The Effect of PTENP1 Overexpression on the Cell Cycle. The cell cycles of Control and PTENP1$^+$ cells with and without TMZ treatment were analyzed by propidium iodide staining and flow cytometry. Data is presented on the histogram as the number of events per fluorescent intensity (on a logarithmic scale), divided by thresholds indicating G0/G1, S, and G2/M phases. (A) The histogram shows the mean fluorescence by event in the Control cells. (B) The histogram shows the mean fluorescence by event in the PTENP1$^+$ cells. (C) The histogram shows the mean fluorescence by event in the Control cells treated with TMZ. (D) The histogram shows the mean fluorescence by event in the PTENP1$^+$ cells treated with TMZ.

PTENP1 overexpression alone and alongside TMZ produced significant effects on cell viability (Figure 7). To further elucidate this change in viability, cell cycle analysis by flow cytometry was performed (Figure 8). PTENP1$^+$ cells induced a 10% increase of cell cycle arrest in both G0/G1 and S phases. Notably, TMZ treatment induced over 80% of both the Control and PTENP1$^+$ cells into G0/G1 phase arrest (Figure 9). PTENP1$^+$ cells treated with TMZ demonstrated a slight increase (~4%) of cells in G2/M phase. Previous reports have indicated that TMZ treatment induces G2/M phase arrest (Barciszewska et al., 2015). This may indicate that PTENP1 overexpression enhanced the mechanism in which TMZ

functions. However, whether the combined effect of PTENP1 overexpression and TMZ treatment is synergistic on cell cycle arrest warrants further investigation. Collectively, PTENP1 overexpression may have produced genotoxic effects, arresting cells in G0/G1 and preventing progression towards mitosis; alongside TMZ, PTENP1 overexpression induced progression towards mitosis.

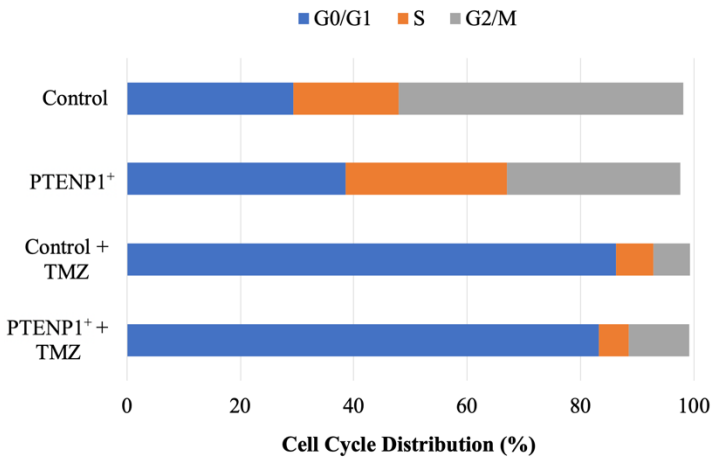

Figure 9: The Effect of PTENP1 Overexpression on Cell Cycle Distribution. The cell cycles of Control, PTENP1$^+$, Control + TMZ, and PTENP1$^+$ + TMZ cells were analyzed by propidium iodide staining and flow cytometry. The percentage of cells in G0/G1 phase were found to be 29%, 38%, 86%, and 83%, respectively. The percentage of cells in S phase were found to be 19%, 29%, 7%, and 5%, respectively. The percentage of cells in G2/M phase were found to be 50%, 30%, 6%, and 11%, respectively.

Increased/Induced Autophagic Cell Death Following PTENP1 Overexpression in Glioma Cells

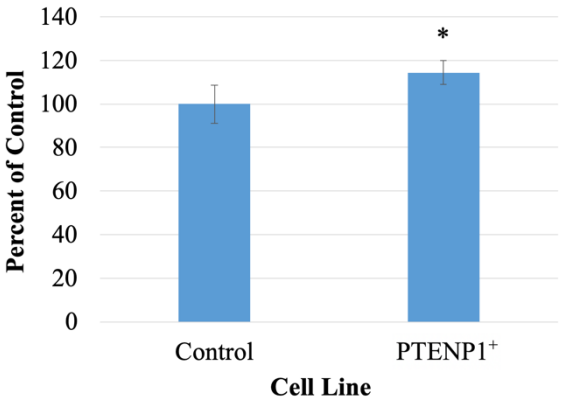

Figure 10: The Effect of PTENP1 Overexpression on phosphorylated LC3. An indirect ELISA was performed to measure pLC3 in Control and PTENP1$^+$ cells. Bars are means +/- STDEV. (n=4). *=p<0.05.

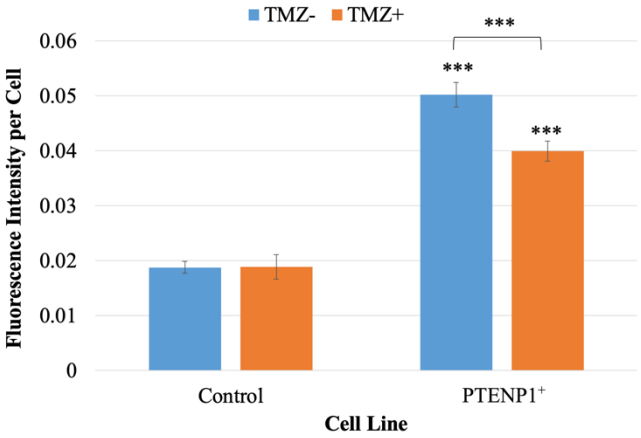

Figure 11. The Effect of PTENP1 Overexpression on Autophagy and Cell Death. Control and PTENP1$^+$ cells with and without TMZ treatment were stained with MDC and PI. MDC detected autophagic vacuole staining intensity with excitation/emission wavelengths of 335/512 nm. PI staining intensity detected the degree of cell death with excitation/emission wavelengths of 536/617 nm. Bars are means +/- STDEV. (n=5). ***=p<0.001.

It has been reported that thalidomide upregulates PTEN and, alongside TMZ, advances cell cycle arrest to G0/G1 phase by inducing autophagy (Gao et al., 2009). Since PTENP1 overexpression upregulated PTEN

levels (Table 3) and induced cell cycle arrest at G0/G1 phase (Figure 9), autophagy was subsequently studied. LC3 is known as an autophagosome marker because LC3-II expression reflects autophagosomes levels (Yoshii & Mizushima, 2017). PTENP1^{+} cells demonstrated increased LC3 expression compared to the Control cells (Figure 10), signifying increased autophagy. To validate the increase in autophagy indicated by LC3, MDC and propidium iodide (PI) staining was quantified to analyze autophagic vacuole and cell death staining intensity, respectively. Compared to untreated Control cells, Control cells treated with TMZ displayed no significant difference in the geometric mean fluorescence intensity (MFI) of MDC staining per live cell. This further validated the MGMT-mediated chemoresistance of the Control cells. With and without TMZ treatment, the PTENP1^{+} cells demonstrated a greater MFI of MDC staining per live cell compared to the Control cells, indicating increased autophagy (Figure 11). While both the Control and PTENP1^{+} cells treated with TMZ demonstrated G0/G1 (Figure 9), only the PTENP1^{+} cells induced autophagy; this suggested that the upregulation of PTEN induced autophagy. Interestingly though, the PTENP1^{+} cells without TMZ demonstrated a greater extent of autophagy compared to PTENP1^{+} cells treated with TMZ. Since the PTENP1^{+} cells treated with TMZ displayed G0/G1 (Figure 9), these data suggested autophagy independent of PTEN; however, this warrants further investigation. Collectively though, autophagy increased with PTENP1 overexpression, with and without TMZ treatment.

Reduced Potential of Angiogenesis Following PTENP1 Overexpression in Glioma Cells

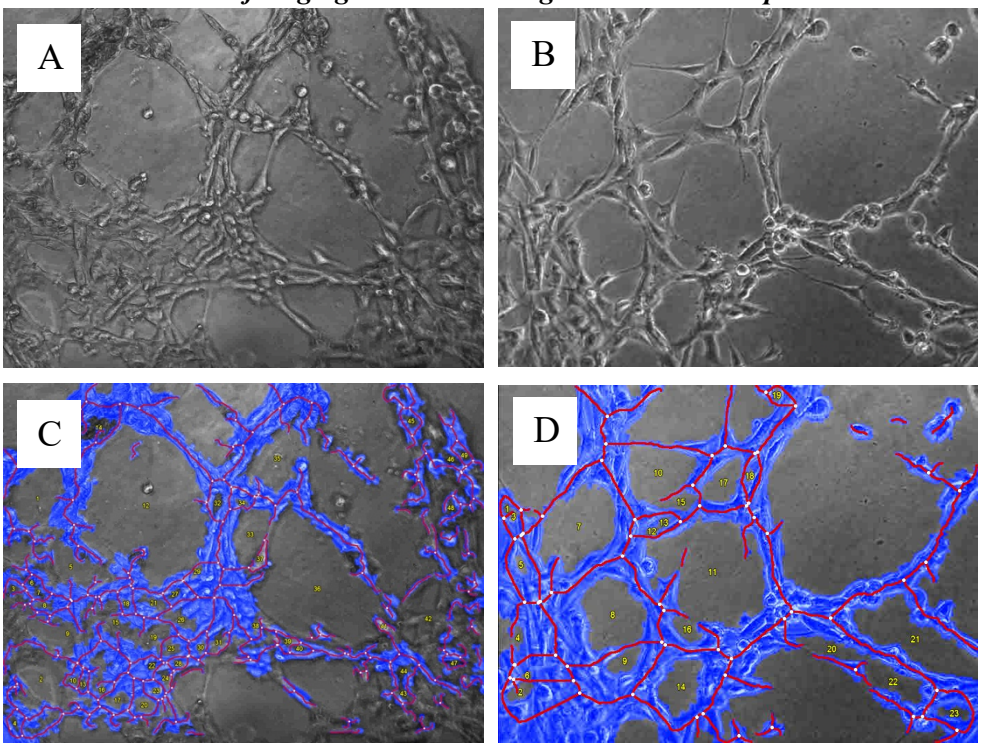

Figure 12: The Effect of PTENP1 Overexpression on Angiogenesis, as shown by Microscopy. A Vascular-Endothelial Tube Formation Assay was performed to visualize and compare the potential of angiogenesis in the (A) Control and (B) PTENP1^{+} cells. Wimasis Image Analysis was utilized to quantify the tube formation in the (C) Control and (D) PTENP1^{+} cells. Cells were imaged at 100X.

PTENP1 overexpression was shown to downregulate miR-26a levels (Table 2). Moreover, it has been reported that miR-26a promotes angiogenesis of endothelial cells (Wang et al., 2019). Therefore, it was of interest to study whether or not PTENP1 had an effect on angiogenesis. A Vascular-Endothelial Tube Formation Assay was performed and the vascular-endothelial tube formations were imaged (Figures 12A and 12B). Quantification of these images (Figures 12C and 12D) revealed a ~60% decrease in the total tube length ($p<0.01$), number of branching points ($p<0.01$), and loops ($p<0.05$) following PTENP1 overexpression (Figure 13). This suggested that PTENP1 overexpression inhibits tube formation, angiogenesis, and potentially metastasis. These findings pertaining to PTENP1 are novel and demonstrate suppression on oncogenic angiogenic capacity in PTENP1$^+$ GBMs. These findings supported Wang et al., 2018 with the reduction of angiogenesis following a decrease in miR-26a.

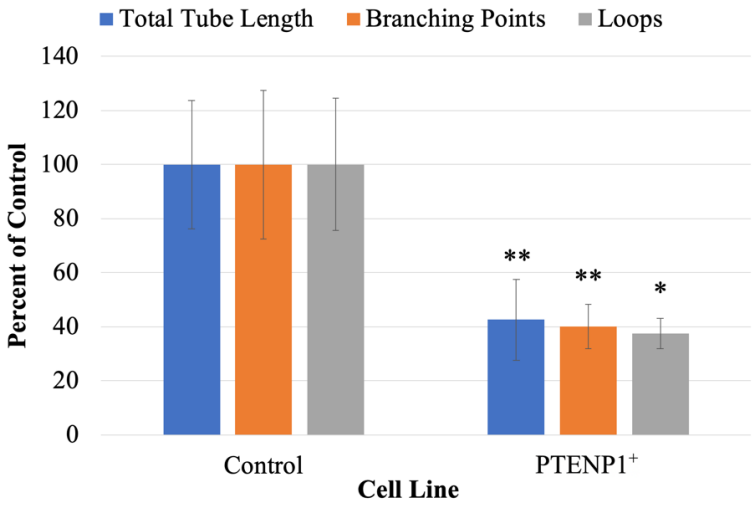

Figure 13: The Effect of PTENP1 Overexpression on Angiogenesis. A Vascular-Endothelial Tube Formation Assay was performed to interpret the potential of angiogenesis in Control and PTENP1$^+$ cells. The total tube length, number of branching points, and number of loops were quantified utilizing Wimasis Image. Bars are means +/- STDEV. (n=4). *=$p<0.05$, **=$p<0.01$.

Inhibition of Migration Following PTENP1 Overexpression in Glioma Cells

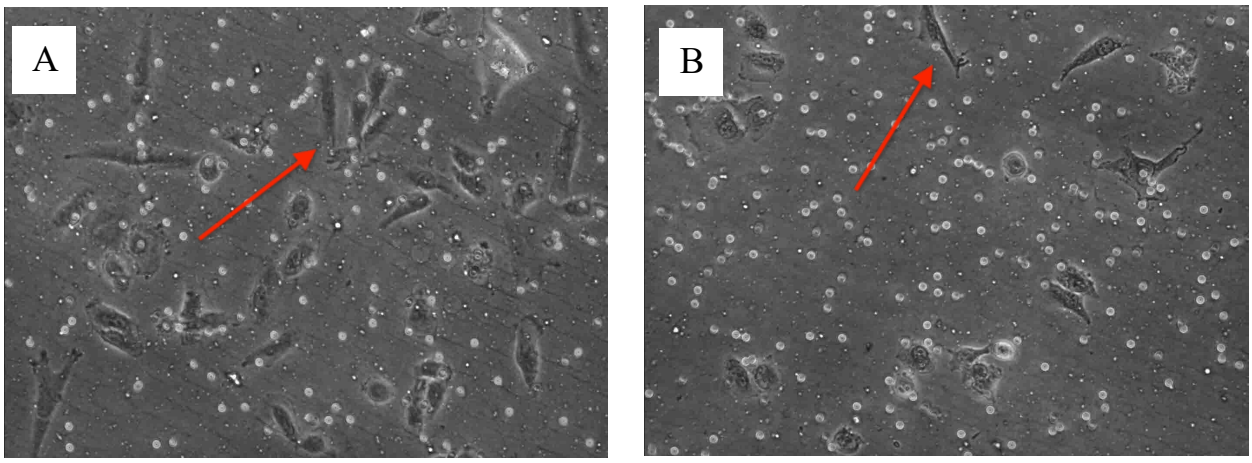

Figure 14: The Effect of PTENP1 Overexpression on Metastasis. A Transwell Migration Assay was performed to visualize and compare the metastatic ability of the (A) Control and (B) PTENP1$^+$ cells. Cells were imaged at 1000X. Migrated cells are indicated by red arrows.

Akt is known to have a role in migration (Wang et al., 2019). Understanding that PTEN antagonizes Akt, it was of interest to investigate how the metastatic process was modulated by PTENP1. A Transwell Migration Assay demonstrated a significant reduction in the migration ability of the PTENP1^{+} cells (Figure 14). This data supported an inhibition of migration independent of FAK levels (Figure 5). Moreover, activation of c-Myc has been observed in stationary compared to migrating glioma cells (Dhruv et al., 2013). Collectively, this demonstrated PTENP1 upregulation inhibited migration.

CONCLUSION

This study proposes and supports PTENP1 upregulation as a novel therapeutic strategy for treating GBMs. PTENP1 overexpression inhibited cell proliferation, enhanced sensitivity to TMZ, induced earlier cell cycle arrest, induced autophagy, and reduced the potential of tube formation modelling angiogenesis, and inhibited migration in GBMs (Figure 15). The mechanism behind PTENP1 overexpression was traced back to decreased miR-26a and was found to subsequently increase PTEN levels. Interestingly though, PTENP1 overexpression upregulated PTEN as well pAkt. This suggested PTEN acts independent of Akt to effectively treat and prevent GBMs (Figure 16). However, the *in vitro* cell culture system is not a model system, as there are no other cells involved and the immune system might have a significant effect. Overall, upregulation of the PTEN pseudogene alongside TMZ treatment is a novel and promising approach in GBMs. The exhibited effects of PTENP1 raises the possibility of dual inhibition and activation of the PI3K/Akt

Characteristic Measured	Assay	Results (Control Cells)	Results (PTENP1^{+} Cells)
PTEN	qRT-PCR	↓	↑
miR-26a	qRT-PCR	↑	↓
PI3K/Akt	Indirect ELISAs	↑	↓↑
Cell Proliferation	MTS	↑	↓
Chemosensitivity	MTS	↓	↑
G0/G1 Arrest	Flow Cytometry	↓	↑
Autophagy	Autophagy	↓	↑
Migration	Migration	↑	↓
Angiogenesis	Tube Formation	↑	↓

Figure 15: Summary of Results. This is a summary of the findings for the assays performed in this study.

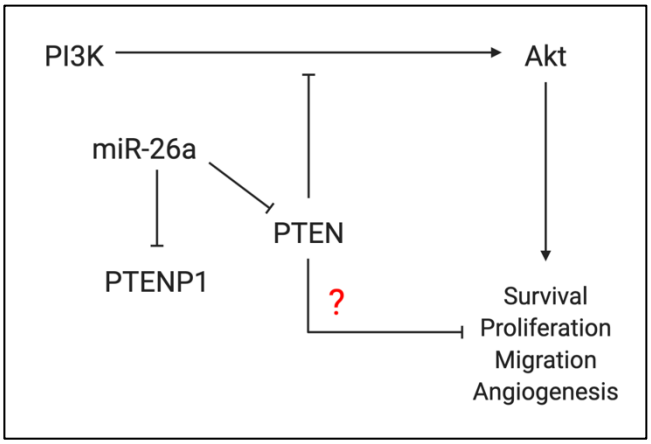

Figure 16: Potential Akt-Independent Mechanism of PTEN. This diagram displays the potential mechanism in which PTEN upregulation inhibited survival, proliferation, migration, and angiogenesis independent of Akt.

pathway as treatment for GBMs, which may necessitate a combinatorial treatment involving a PI3K/Akt inhibitor.

Future research can involve further investigation underlying PI3K/Akt pathway modulation in different compartments within the cell. Currently, there is scant information detailing the mechanism in which the sense and antisense PTENP1 transcripts affect GBMs. Moreover, it has reported that diffuse large B-cell lymphomas with high cytoplasmic expression of PTEN are associated with higher nuclear pAkt levels (Wang et al. 2018); by the same token, PTENP1 overexpression in GBMs may have selectively mediated the PI3K/Akt pathway based on cellular location of the PTENP1 transcript. Hence, further research could study the potential of PI3K/Akt pathway expression "gradients" between different cellular compartments in treating GBMs.

REFERENCES

Barciszewska, Anna-Maria & Gurda, Dorota & Głodowicz, Paweł & Nowak, Stanisław & Naskręt-Barciszewska, Mirosława. (2015). A New Epigenetic Mechanism of Temozolomide Action in Glioma Cells. PloS one. 10. e0136669. 10.1371/journal.pone.0136669.

Chen, C. Y., Chang, J. T., Ho, Y. F., & Shyu, A. B. (2016). MiR-26 down-regulates TNF-α/NF-κB signalling and IL-6 expression by silencing HMGA1 and MALT1. *Nucleic acids research*, *44*(8), 3772–3787. doi:10.1093/nar/gkw205.

Chen, H., Liu, H. & Qing, G. Targeting oncogenic Myc as a strategy for cancer treatment. *Sig Transduct Target Ther* 3, 5 (2018) doi:10.1038/s41392-018-0008-7

De Salvo, M., Maresca, G., D'agnano, I., Marchese, R., Stigliano, A., Gagliassi, R., … Bucci, B. (2011). *Temozolomide induced c-Myc-mediated apoptosisviaAkt signalling in MGMT expressing glioblastoma cells. International Journal of Radiation Biology, 87(5), 518–533.* doi:10.3109/09553002.2011.556173.

Dhruv, H. D., McDonough Winslow, W. S., Armstrong, B., Tuncali, S., Eschbacher, J., Kislin, K., … Berens, M. E. (2013). Reciprocal activation of transcription factors underlies the dichotomy between proliferation and invasion of glioma cells. *PloS one*, *8*(8), e72134. doi:10.1371/journal.pone.0072134.

Gao, Song & Yang, Xuejun & Zhang, Wen-gao & Ji, Yan-wei & Pan, Qiang. (2009). Mechanism of thalidomide to enhance cytotoxicity of temozolomide in U251-MG glioma cells in vitro. Chinese medical journal. 122. 1260-6. 10.3760/cma.j.issn.0366-6999.2009.11.005.

Ge, X., Pan, M., Wang, L. *et al.* Hypoxia-mediated mitochondria apoptosis inhibition induces temozolomide treatment resistance through miR-26a/Bad/Bax axis. *Cell Death Dis* 9, 1128 (2018) doi:10.1038/s41419-018-1176-7.

Goc, A., Al-Husein, B., Katsanevas, K., Steinbach, A., Lou, U., Sabbineni, H., … Somanath, P. R. (2014). Targeting Src-mediated Tyr216 phosphorylation and activation of GSK-3 in prostate cancer cells inhibit prostate cancer progression in vitro and in vivo. *Oncotarget*, *5*(3), 775–787. doi:10.18632/oncotarget.1770.

Guo, P., Nie, Q., Lan, J., Ge, J., Qiu, Y., & Mao, Q. (2013). C-Myc negatively controls the tumor suppressor PTEN by upregulating miR-26a in glioblastoma multiforme cells. Biochemical and Biophysical Research Communications, 441(1), 186–190. doi:10.1016/j.bbrc.2013.10.034 .

Haddadi, N., Lin, Y., Travis, G., Simpson, A. M., Nassif, N. T., & McGowan, E. M. (2018). PTEN/PTENP1: 'Regulating the regulator of RTK-dependent PI3K/Akt signalling', new targets for cancer therapy. *Molecular cancer*, *17*(1), 37. doi:10.1186/s12943-018-0803-3.

Hill, V. K., Kim, J. S., James, C. D., & Waldman, T. (2017). Correction of PTEN mutations in

glioblastoma cell lines via AAV-mediated gene editing. *PloS one*, *12*(5), e0176683. doi:10.1371/journal.pone.0176683.

Huse, J. T., Brennan, C., Hambardzumyan, D., Wee, B., Pena, J., Rouhanifard, S. H., … Holland, E. C. (2009). The PTEN-regulating microRNA miR-26a is amplified in high-grade glioma and facilitates gliomagenesis in vivo. *Genes & development*, *23*(11), 1327–1337. doi:10.1101/gad.1777409.

Johnsson, P., Ackley, A., Vidarsdottir, L., Lui, W. O., Corcoran, M., Grandér, D., & Morris, K. V. (2013). A pseudogene long-noncoding-RNA network regulates PTEN transcription and translation in human cells. *Nature structural & molecular biology*, *20*(4), 440–446. doi:10.1038/nsmb.2516.

Kotliarova, S., Pastorino, S., Kovell, L. C., Kotliarov, Y., Song, H., Zhang, W., … Fine, H. A. (2008). Glycogen synthase kinase-3 inhibition induces glioma cell death through c-MYC, nuclear factor-kappaB, and glucose regulation. *Cancer research*, *68*(16), 6643–6651. doi:10.1158/0008-5472.CAN-08-0850.

Langhans, J., Schneele, L., Trenkler, N., von Bandemer, H., Nonnenmacher, L., Karpel-Massler, G., … Westhoff, M. A. (2017). The effects of PI3K-mediated signalling on glioblastoma cell behaviour. Oncogenesis, 6(11), 398. doi:10.1038/s41389-017-0004-8.

Lezina, L., Purmessur, N., Antonov, A. V., Ivanova, T., Karpova, E., Krishan, K., … Barlev, N. A. (2013). miR-16 and miR-26a target checkpoint kinases Wee1 and Chk1 in response to p53 activation by genotoxic stress. *Cell death & disease*, *4*(12), e953. doi:10.1038/cddis.2013.483.

Li, M., Liang, R. F., Wang, X., Mao, Q., & Liu, Y. H. (2017). BKM120 sensitizes C6 glioma cells to temozolomide via suppression of the PI3K/Akt/NF-κB/MGMT signaling pathway. *Oncology letters*, *14*(6), 6597–6603. doi:10.3892/ol.2017.7034.

Li, Q., Wang, A. Y., Xu, Q. G., Liu, D. Y., Xu, P. X., & Yu, D. (2015). In-vitro inhibitory effect of EGFL7-RNAi on endothelial angiogenesis in glioma. *International journal of clinical and experimental pathology*, *8*(10), 12234–12242.

Liu, B., Li, J., & Cairns, M. J. (2014). Identifying miRNAs, targets and functions. *Briefings in bioinformatics*, *15*(1), 1–19. doi:10.1093/bib/bbs075.

Mao, Maiya J, and Donna E Leonardi. “Vascular-endothelial response to IDH1 mutant fibrosarcoma secretome and metabolite: implications on cancer microenvironment.” *American journal of cancer research* vol. 9,1 122-133. 1 Jan. 2019.

Rüegger, S., & Großhans, H. (2012). MicroRNA turnover: when, how, and why. Trends in Biochemical Sciences, 37(10), 436–446. doi:10.1016/j.tibs.2012.07.002.

Wang, X., Cao, X., Sun, R., Tang, C., Tzankov, A., Zhang, J., … Young, K. H. (2018). Clinical.

Significance of PTEN Deletion, Mutation, and Loss of PTEN Expression in De Novo Diffuse Large B- Cell Lymphoma. *Neoplasia (New York, N.Y.)*, *20*(6), 574–593. doi:10.1016/j.neo.2018.03.002

Wang, Z., Liao, F., Wu, H. *et al.* Glioma stem cells-derived exosomal miR-26a promotes angiogenesis of microvessel endothelial cells in glioma. *J Exp Clin Cancer Res* 38, 201 (2019) doi:10.1186/s13046-019-1181-4.